Journal of Applied Polymer Science

Selective Preparation of Carbon Nanoflakes, Carbon Nanospheres, and Carbon Nanotubes Through Carbonization of Polymethacrylate by Using Different Catalyst Precursors

Ningning Hong,[1] Gang Tang,[1] Xiaofeng Wang,[1] WeiZhao Hu,[1] Lei Song,[1] Yuan Hu[1,2]

[1]State Key Laboratory of Fire Science, University of Science and Technology of China, Hefei, Anhui 230026, People's Republic of China

[2]Suzhou Key Laboratory of Urban Public Safety, Suzhou Institute of University of Science and Technology of China, Suzhou, Jiangsu, 215123, People's Republic of China

Correspondence to: Y. Hu (E - mail: yuanhu@ustc.edu.cn) or L. Song (leisong@ustc.edu.cn).

ABSTRACT: This work reports the selective preparation of different kinds of carbon nanomaterials through carbonization of polymethacrylate (PMA)/organophilic clay (Oclay) composite by just changing the catalyst precursors. The morphologies and structures of the carbon materials were characterized by Scanning and Transmission electron microscopy, X-ray diffraction, Raman spectroscopy, Fourier transform infrared spectroscopy and X-ray photoelectron spectroscopy. The result indicated that the catalyst precusors had a strong influence on the morphologies and yields of the obtained products. Carbon nanoflakes were produced when iron oxide was used as the catalyst precursor, cobalt oxide favored the formation of carbon nanospheres, while carbon nanotubes occurred over nickel oxide. The presence of Oclay plallets was determined to prevent the pyrolytic carbon species of PMA in the system from escaping, thus relatively more carbon nanomaterials were obtained. Based on the experimental observations, a possible mechanism was discussed for illustrating the growth process. © 2013 Wiley Periodicals, Inc. J. Appl. Polym. Sci. 130: 1029–1037, 2013

KEYWORDS: catalysts; clay; degradation; morphology; nanotubes; graphene and fullerenes

Received 20 December 2012; accepted 3 March 2013; published online 17 April 2013
DOI: 10.1002/app.39241

INTRODUCTION

Since the discovery of fullerene in 1985,[1] much attention has been paid to the carbon nanomaterials with various special shapes and structures. Typical forms of carbon nanomaterials, such as two dimensional (2D) carbon nanoflakes (CNFs) or graphene, 0D carbon nanospheres (CNSs), and 1D carbon nanotubes (CNTs) have attracted huge interest due to their promising application in the fields of catalysis, energy conversion and storage, and biomedical science.[2–4] Recently, because of their plenty use in matrices as reinforcing materials,[5–9] the demands on the low cost, large scale of CNFs, CNSs, and CNTs with sacrificing part of high quality become more and more urgent. Up to date, CNFs are usually prepared by microwave plasma enhanced chemical vapor deposition (CVD) and radio-frequency inductively coupled CVD.[10,11] Previous methods used to produce CNSs contain CVD, mixed-valent oxide catalytic carbonization and self-generated template approach.[12–14] As the acquisition of CNTs by arc discharge, several routes such as laser vaporization and CVD have been explored to prepare CNTs in large quantities.[15,16] However, most of the methods mentioned have limitations in term of economic production and safety consideration because of the harsh synthetic conditions. Recently, carbonization of common solid carbon sources has been considered as a cost-effective and sustainable process to fabricate carbon nanomaterials, as it could reduce the experimental requirements to a great extent. Pyrolysis of solid carbon sources including camphor,[17] phthalocyanine[18] and poly(methyl methacrylate)[19] provides a new way for the low cost and facile production of carbon nanoflakes. CNSs converted from polymers such as polyethylene terephthalate,[20] polycarbynes,[21] and other waste plastics[22] makes the preparation of carbon spheres more cost-effective and simplified. Polypropylene[23,24] and poly(vinyl alcohol)[25] used as carbon sources to synthesize CNTs pays a promising way for the large-scale production of CNTs.

Although conversion of solid sources into carbon nanomaterials is a great progress compared to the traditional methods in an economic viewpoint, there is barely a facile and selective method for the fabrication of carbon nanomaterials with a desired morphology. Qi et al. reported the synthesis of carbon nanofibers, bamboo-like carbon nanotubes, and chains of

carbon nanospheres in large scale as the temperature varied from 500 to 700°C.[26] It is very charming that selective synthesis of CNFs, CNSs and CNTs is controlled by changing only few parameters such as temperature, carbon source or catalyst. As is well known, a single layer of graphite is the starting material for consisting the family of graphitic carbon. It is crucial to control the early stage of nucleation of graphene as it can be rolled into 1D nanotubes or stacked into 2D graphene or bent into 0D carbon nanospheres.

Based on the deep understanding of the formation mechanism of graphene, CNSs and CNTs, we provide a simple method for the selective preparation of carbon nanomaterials with different shapes by pyrolyzing polymethacrylate (PMA) using different catalyst precursors. Common polymer of PMA herein is used as carbon source because it can be easily pyrolyzed into various carbon species. And also, it shows great advantages in consideration of its low cost and facile availability. CNFs are produced when iron oxide (Fe_2O_3) is used as the catalyst, CNSs are obtained in the presence of cobalt oxide (Co_3O_4), and the incorporation of nickel oxide (NiO) leads to the formation of CNTs. The obtained products are characterized by transmission electron microscopy (TEM), scanning electron microscopy (SEM), X-ray diffraction (XRD), Raman spectroscopy, Fourier Transform Infrared Red spectroscopy (FTIR) and X-ray photoelectron spectroscopy (XPS). The possible formation procedure of CNFs, CNTs and CNTs is discussed on the basis of the experimental observations.

EXPERIMENTAL

Materials

Methacrylate (MA) bought from Sinopharm Chemical Reagent was refined before use. Benzoyl peroxide (BPO) used as initiator was provided by Sinopharm Chemical Reagent Co., Ltd. Organophilic clay (Oclay) was kindly provided by Keyan company (Anhui, China). Fe_2O_3, Co_3O_4 and NiO were separately prepared through co-precipitation of metal nitrate and urea aqueous solution and subsequent transformation of metal hydroxide into metal oxide by thermal calcination at 400 °C.[27]

Preparation of PMA Composites

In a 100 mL three-necked flask was placed 18 g MA, 1 g Oclay and 0.036 g BPO as radical initiator. This mixture was stirred at room temperature under flowing nitrogen gas until it became homogeneous, and then was heated to 85°C for a few minutes to prepolymerize. 1 g Fe_2O_3, Co_3O_4 or NiO nanoparticles was separately added and the reaction was stirred until a critical viscosity of the system was reached. The viscous mixture was then placed into an oven at 50 °C for 48 h to complete the polymerization process.

Carbonization of PMA Composites into CNFs, CNSs, and CNTs

The experiment was carried out in a tube furnace equipped with a quartz tube of around 120 cm in length and 30 mm in diameter. After the introduction of a flow of nitrogen, weighed sample was inserted into the quartz tube, which was then placed inside the tube furnace. The carbonization disposal was performed from room temperature to 850 °C at a rapid heating rate and then maintained at 850 °C for 15 min. After the reaction, the reactor was quickly cooled under nitrogen flow. The collected black powders were purified in a mixed solution of dilute hydrofluoric acid and nitric acid at room temperature for 5 h. After filtration and washing, the purified products were dried in oven at 80 °C.

Characterization

TEM micrographs were obtained by JEOL 2010 with an acceleration voltage of 200 kV. Specimens for the high resolution TEM (HRTEM) measurements were obtained by dispersing the powdery material in ethanol using an ultrasonic bath. A drop of the suspension was placed onto a lacy carbon film supported by a Cu grid. SEM micrographs were taken by using a JSM-6800F scanning electron microscope produced by JEOL. The char was adhered on the copperplate, and then coated with gold/palladium alloy ready for imaging. Raman spectroscopy measurement was carried out at room temperature with a SPEX-1403 laser Raman spectrometer (SPEX). FT-IR spectroscopy (Nicolet 6700 FT-IR spectrophotometer) was employed to characterize the synthesized product using thin KBr disc. The transition mode was used and the wave number range was set from 4,000 to 500 cm^{-1}. XPS was recorded using a Kratos Axis Ultra-DLD spectrometer employing a monochromatic Al Kα X-ray source ($h\nu$ = 1,486.6 eV), hybrid (magnetic/electrostatic) optics and a multichannel plate and delay line detector. A Govmark MCC-2 microscale combustion calorimetry (MCC) was used to determine the flammability characteristics of composites according to ASTM D 7309-07. About 5 mg specimens were thermally decomposed in an oxygenated environment at a constant heating rate of 3 K/s. XRD patterns were performed with a Japan Rigaku D/Max-Ra rotating anode X-ray diffractometer equipped with a Cu-Ka tube and Ni filter (λ = 0.1542 nm).

RESULTS AND DISCUSSION

The phase compositions and morphologies of as-prepared catalyst precursors were characterized by XRD and SEM as shown in Figure 1. From Figure 1(a), it shows all diffraction peaks that are well indexed to α-Fe_2O_3 and no other impurity peak is observed. The SEM image of the synthesized Fe_2O_3 is shown in Figure 1(b). The product is composed of microspheres with an average size of 400–600 nm. The typical diffraction detected in Figure 1(c) indicates that the Co_3O_4 is successfully synthesized. The product shows a spherical shape with a wide size distribution and the big particles are the aggregation of nanoparticles Figure 1(d). Figure 1(e) shows the sharp peaks, and no visible impurity peaks indicates the high purity of NiO catalyst precursor. As shown in Figure 1(f), the NiO owns nanosphere-like morphology and tends to aggregate into big particles.

TEM was used to characterize the microstructures of the purified products obtained via the pyrolysis method. Figure 2 displays the TEM images of the purified residues by pyrolyzing PMA/Oclay composite using Fe_2O_3, Co_3O_4 and NiO as the catalysts. When Fe_2O_3 is used as the catalyst, crumpled carbon sheets stacked over one another are observed [Figure 2(a)]. More specifically, the HRTEM image viewing at the edge of a flake, indicates that the flake is consisted of few graphitic layers

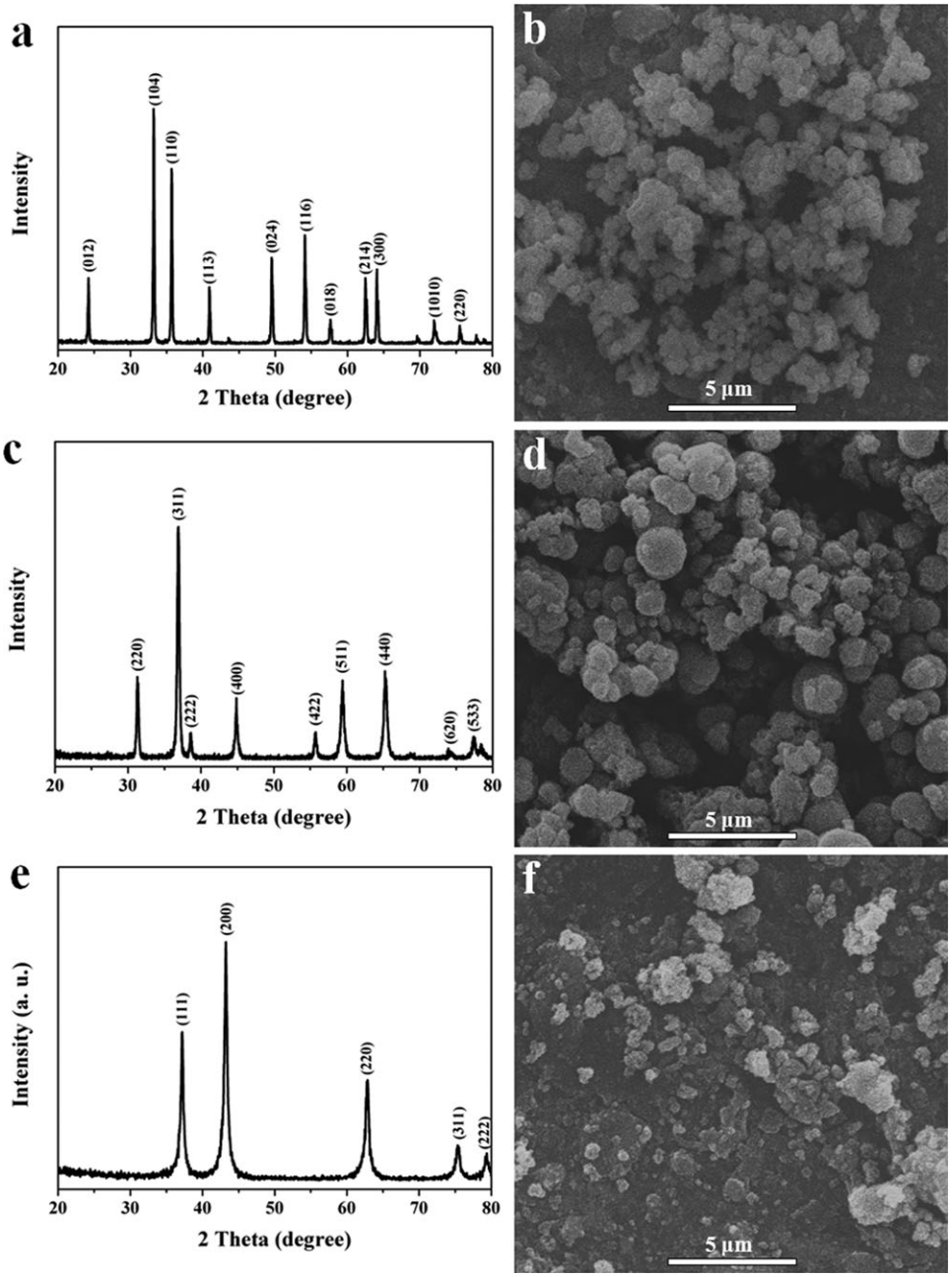

Figure 1. XRD patterns and SEM images of as-prepared Fe_2O_3 (a, b), Co_3O_4 (c, d) and NiO (e, f).

with the distance of about 0.34 nm [Figure 2(d)]. When Co_3O_4 is selected as the catalyst, numerous spheres with both core–shell structure and hollow structure are found in the final product [Figure 2(b)]. From the HRTEM image of the carbon nanospheres, it is found that the carbon shells of the nanospheres have ordered graphitic layers with the interspacing of about 0.37 nm [Figure 2(e)]. If NiO is chosen as the catalyst, large bundles of closely packed carbon nanotubes could be obtained [Figure 2(c)]. As shown in Figure 2(f), the CNTs are composed of many parallel cylindrical graphitic layers. The lattice fringe spacing of the graphitic layers is estimated to be 0.34 nm.

The system composition plays an important role in the formation procedure of the carbon nanomaterials. SEM was used to observe the morphology of the carbon nanomaterials prepared from carbonization of PMA/Oclay (a), PMA/Oclay/Fe_2O_3 (b), PMA/Oclay/Co_3O_4 (c), and PMA/Oclay/NiO (d) respectively. As shown in Figure 3(a), mainly amorphous carbon was observed in the sample through carbonization of PMA/Oclay composite. After the addition of Fe_2O_3 catalyst, the carbonization of the composite leads to the formation of thin carbon sheets with lateral thicknesses less than 8 nm and size dimension up to several micrometers [Figure 3(b)]. With regard to the PMA/Oclay/

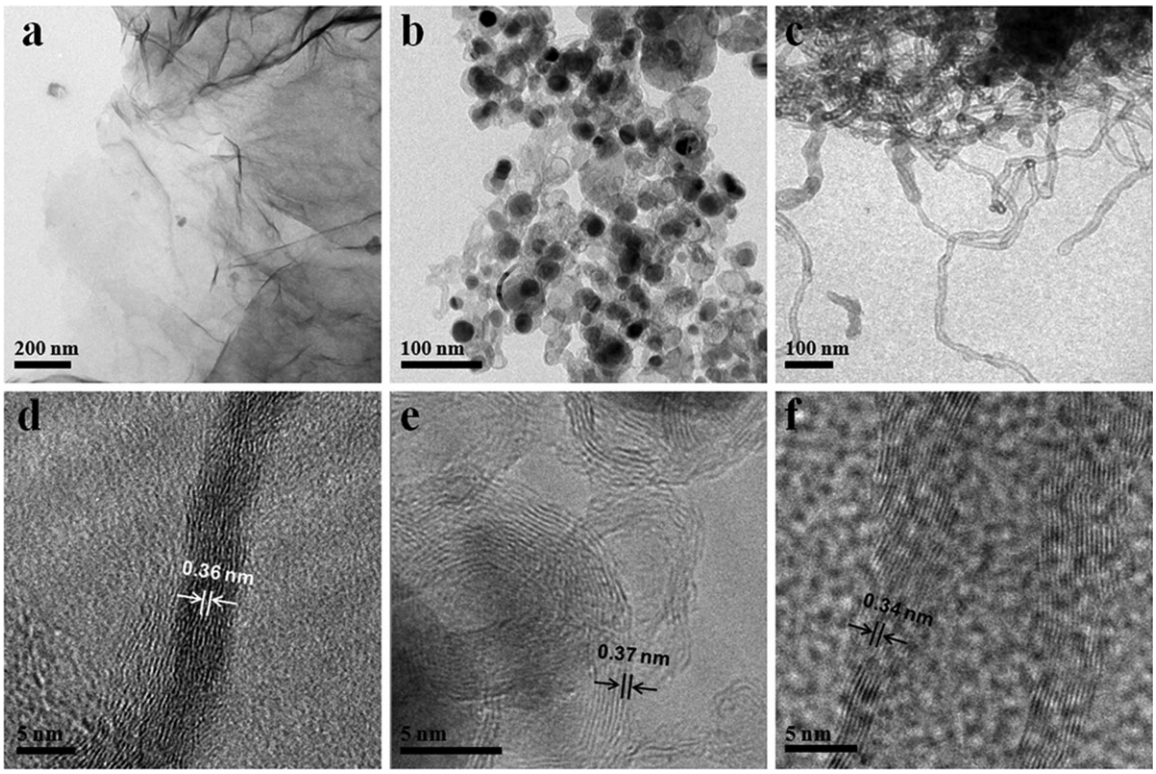

Figure 2. TEM and HRTEM images of the purified carbon materials obtained from carbonization of PMA/Oclay composite by using Fe_2O_3 (a, d), Co_3O_4 (b, e) and NiO (c, f) as the catalyst precursors.

Co_3O_4 composite, the final char is actually spherical carbon nanoparticles with diameters between 25 and 50 nm [Figure 3(c)]. As revealed in Figure 3(d), the residual sample is composed of large numbers of long fiber-like structure by pyrolysis of PMA/Oclay/NiO composite. The result indicates that the type of catalyst is a critical factor determining the morphology of final product.

Raman spectroscopy is a powerful tool to estimate the crystallinity of the as-prepared products, especially for the carbonaceous materials. The Raman spectra of the different samples (Figure 4) all show two prominent peaks of the *D* (originated from the defects or structural disorder) and *G* band (ascribed to the bond stretching between pairs of sp^2) located at around 1,350 and 1,600 cm^{-1}, respectively. The intensity ratio of I_G to I_D is an important parameter to measure the graphitization degree of carbon structures.[28,29] Based on the Raman spectra, the calculated I_G/I_D value for amorphous carbon, CNFs, CNSs and CNTs is 0.523, 0.545, 0.597, and 0.609 respectively, indicating the existence of some disordered structures in the carbon nanomaterials obtained by the pyrolytic method. The graphitic degree of amorphous carbon is the lowest, while that of CNTs grown by using NiO catalyst is the highest. The graphitic degree of CNSs grown by using Co_3O_4 catalyst is higher than that of CNFs grown by using Fe_2O_3 catalyst. These results are a little different with the reported result.[30]

FT-IR was employed to investigate the chemical and structural information of carbon materials obtained by this method. The band at 3,438 cm^{-1} assigned to O—H stretching, and the peaks at 2,920 and 2,850 cm^{-1} corresponding to —CH_3 and —CH_2 were observed in Figure 5(a), indicative of the existence of disordered structure. The characteristic peaks at 1,588 cm^{-1} for CNFs, CNSs and CNTs were attributed to C=C stretching arised from the formed graphitic structure. The carbon nanomaterials also exhibit other absorption bands at 1,718 cm^{-1} due to the C=O stretching as well as bands due to carboxy C—O (1,385 cm^{-1}) and epoxy C—O (1,167 cm^{-1}). The result is similar to that has been reported previously.[31] XPS analysis was employed to determine elemental compositions of three carbon materials. Both the carbon and oxygen elements are found in the XPS spectra of the final products because they are originated from the structure of raw carbon source. Calculated from XPS data, the atomic percentage of oxygen in the as-prepared carbon materials is found to be less than 4.4%. High-resolution C1s XPS spectra are shown in the insets of Figure 5(b–d). A sharp peak at 284.5 eV is assigned to sp^2-hybridized C (C=C) and the weak peak at 285.6 eV corresponding to the sp^3-carbon (C—C) is also observed for the C1s peak.[32] The peak intensity of the former is higher than that of the latter, indicating the high degree of graphitization of the prepared carbon materials. Moreover, two weak peaks observed at 286.8 and 288.7 eV could be attributed to C—O—C and O=C—O group arising from epoxide, ether, and carboxyl groups.[33]

To make sure the role that Oclay plays in the pyrolysis process, microscale combustion calorimeter (MCC) test of PMA and PMA/Oclay was performed [Figure 6(a)]. MCC is a rapid and useful method to evaluate the flammability of materials, which

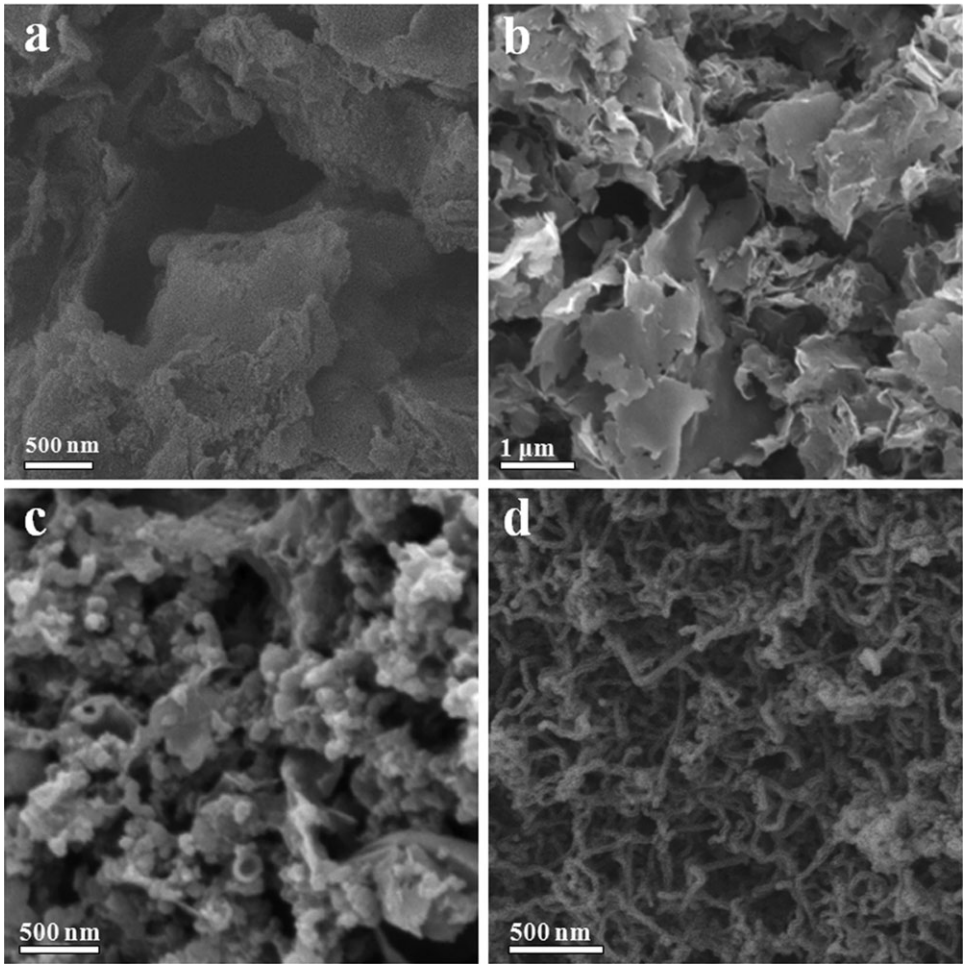

Figure 3. SEM images of the samples obtained from carbonization of PMA/Oclay (a) and PMA/Oclay/Fe_2O_3 (b), PMA/Oclay/Co_3O_4 (c), and PMA/Oclay/NiO (d).

is based on measuring the heat of combustion of the gases evolved during controlled pyrolyzing the samples in nitrogen.[34] Seen from Figure 6(a), the combustion time of PMA/Oclay prolongs to 141 s that is larger than 133 s of the pure PMA. The peak heat release rate of PMA is decreased after the addition of 5 wt % Oclay. The experimental results reveal that fewer combustable gaseous species are formed during the pyrolysis of PMA due to the existence of Ocaly. The char yields of PMA and PMA/Ocaly after pyrolysis are listed in Figure 6(b). With the absence of Oclay, there is almost nothing left after the pyrolysis of PMA. The addition of Oclay is beneficial for increasing the char yield of PMA to 13 wt %, indicating that Oclay could enhance the carbonization of PMA in the thermal pyrolysis process and reduce the mass loss rate. There are already several reports about the effect of clay on improving char yield of polymers during combustion because of its gas barrier properties.[35] Therefore, it is concluded herein that thermally stable Oclay pallets could act as superior insulators during combustion which would prevent pyrolytic species of PMA from escaping and thus more char residues are left.[36]

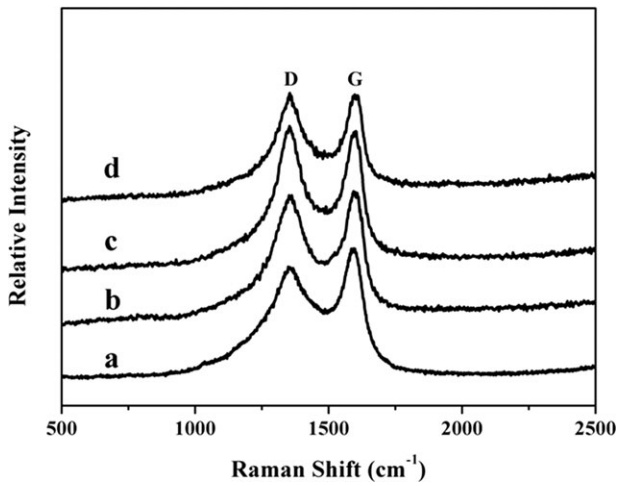

Figure 4. Raman spectra of the carbon materials obtained from carbonization of PMA/Oclay (a) and PMA/Oclay/Fe_2O_3 (b), PMA/Oclay/Co_3O_4 (c), and PMA/Oclay/NiO (d).

To understand the formation mechanism of CNFs, CNSs, and CNTs, the pyrolysis process was performed in a short reaction time with other conditions keeping unchanged to explore the structure evolution of graphene at the initial stage. XRD was employed to characterize the raw charred residues obtained through carbonization of PMA composites. When Fe_2O_3 is

Applied Polymer SCIENCE

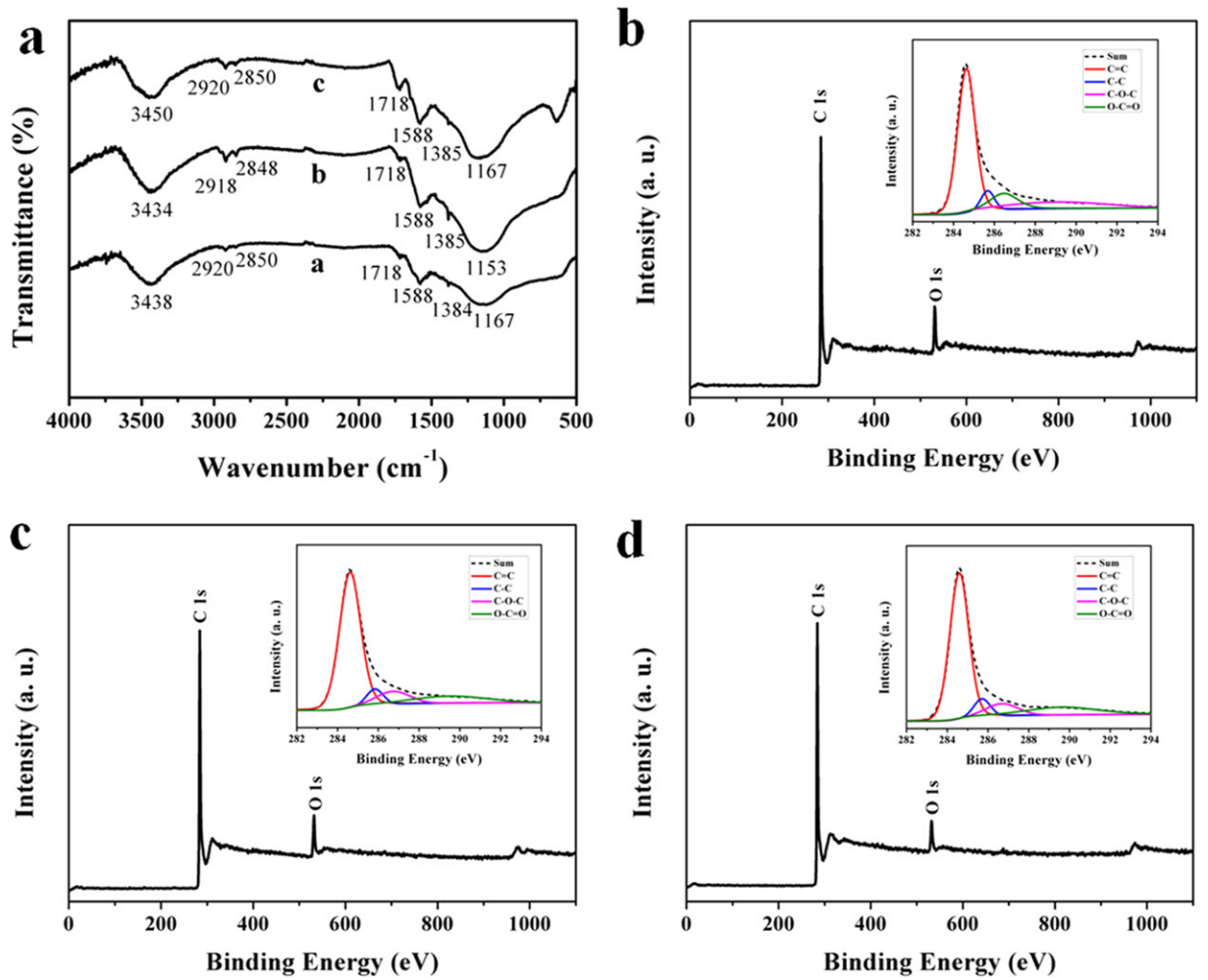

Figure 5. (a) FTIR spectrum of CNFs, CNSs, and CNTs, and survey XPS spectra spectra of CNFs (b), CNSs (c), and CNTs (d). The inset in panel b, c and d is the corresponding C1s XPS spectra. [Color figure can be viewed in the online issue, which is available at wileyonlinelibrary.com.]

used, the XRD pattern of raw product is displayed in Figure 7(a). The strong peaks appearing at 44.69° and 65.06° originate from the diffraction of (110) and (200) planes of Fe with high crystallinity. This means that Fe nanoparticles are in situ formed from the reduction of Fe_2O_3 by the reductive pyrolytic species of PMA, which play the role of the active sites for the formation

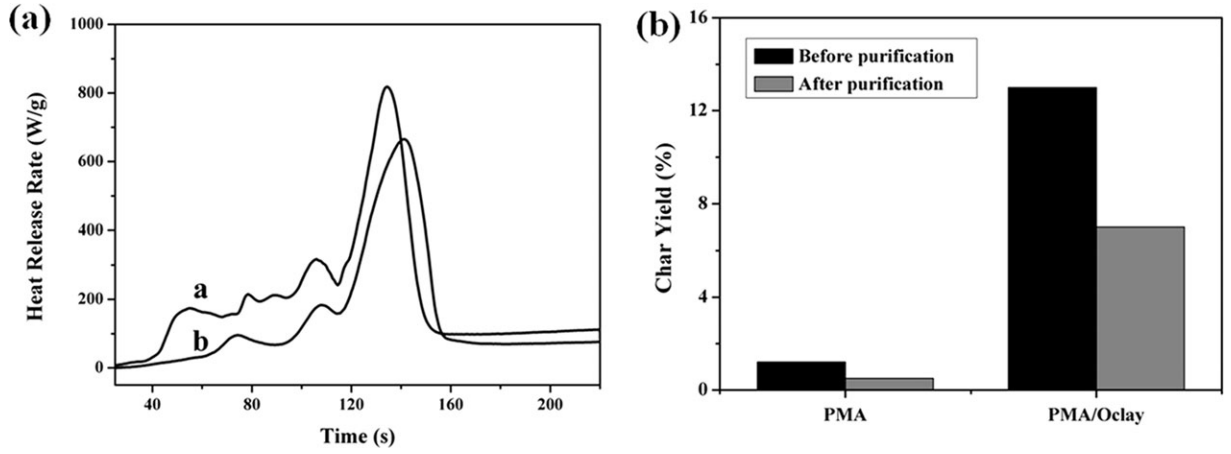

Figure 6. (a) MCC curves of PMA and PMA/Oclay composite and (b) char yields of PMA composites after pyrolysis. The inset in panel a is the TEM image of the raw char residue of PMA/Oclay.

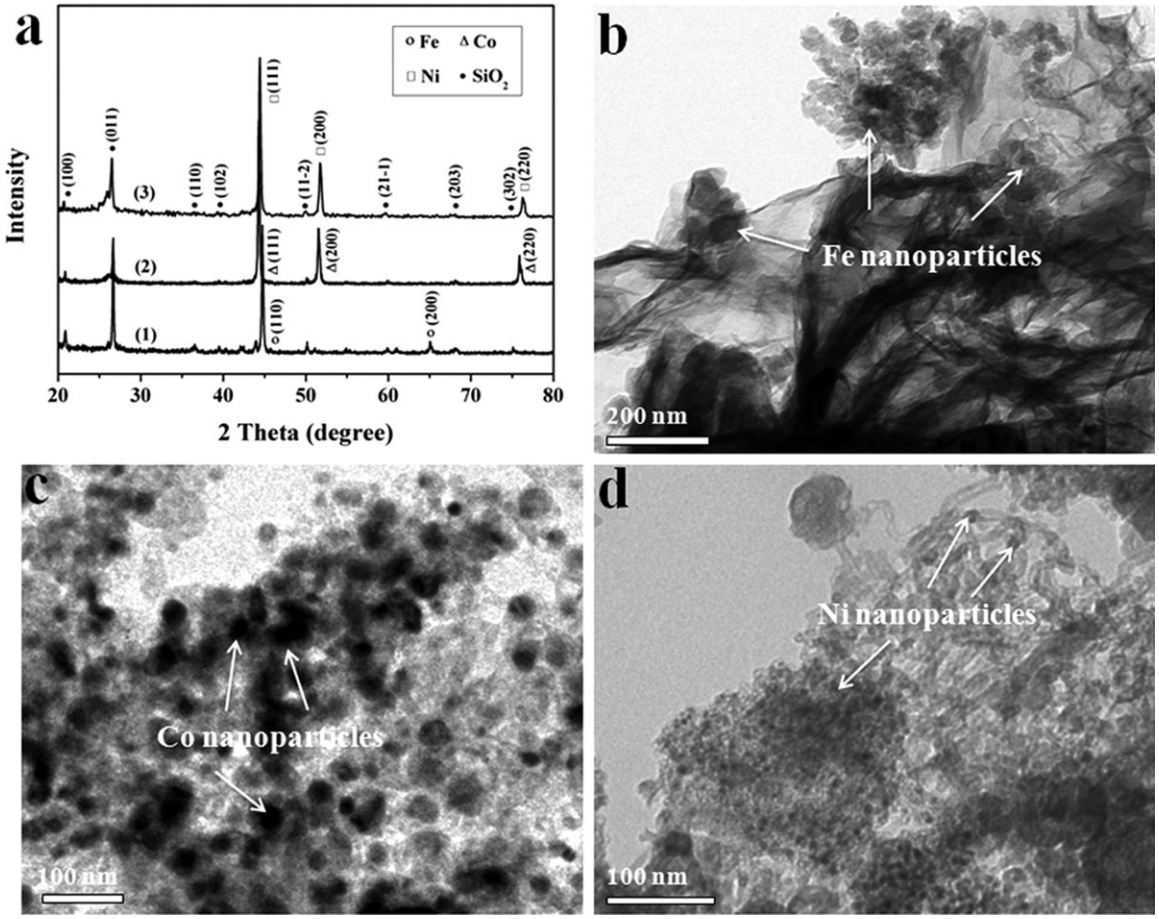

Figure 7. (a) XRD patterns of the raw char residues of PMA/Oclay/Fe_2O_3 (1), PMA/Oclay/Co_3O_4 (2) and PMA/Oclay/NiO (3), and TEM images of the raw char residues by pyrolysis of PMA/Oclay/Fe_2O_3 (b), PMA/Oclay/Co_3O_4 (c), and PMA/Oclay/NiO (d).

of CNFs. As for Co_3O_4 and NiO catalyst, the same case also occurs. Co_3O_4 and NiO are immediately reduced to Co and Ni nanoparticles during the process, which then catalyze the pyrolytic species into GNSs and CNTs [Figure 7(a)] respectively. Another peak identified at around 26.5° for all the samples is ascribed to silica formed from thermal decomposition of Oclay. The diffraction area ascribed to the graphitic carbon may somewhat overlap with that of silica. The initial growth stages of carbon nanomaterials using different catalysts were established by TEM measurements, as revealed in Figure 7. As for Fe_2O_3 catalyst, the formation of thin sheets like graphene covering Fe nanoparticles is easily observed [Figure 7(b)]. With regard to Co_3O_4 catalyst, the product is almost composed of nanospheres with core-shell structures. Each nanosphere with the shell being

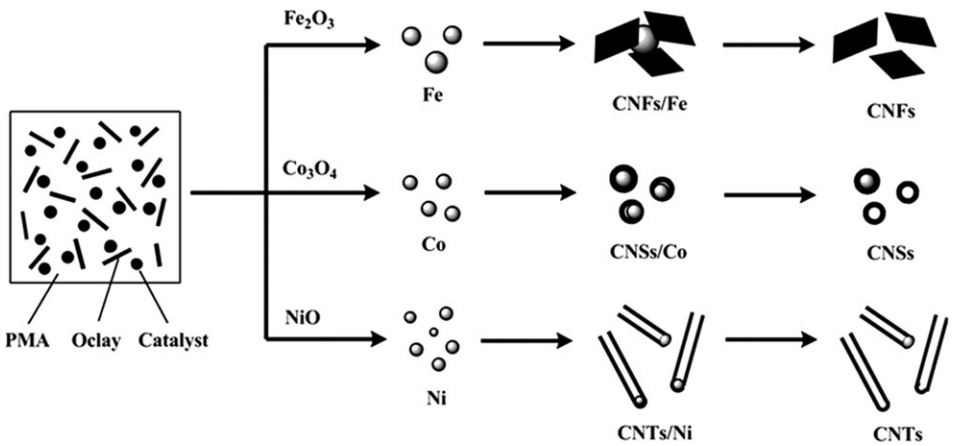

Figure 8. Schematic illustration for the formation procedures of CNFs, CNSs, and CNTs.

graphite and the core containing Co is demonstrated from the XRD pattern. The diameters of the inner Co nanoparticles are ranging from 10 to 25 nm [Figure 7(c)]. In the case of using NiO catalyst, abundance of CNTs with globose Ni nanoparticles at the tips are observed throughout the sample [Figure 7(d)]. The formed Ni nanoparticles have narrow diameter distributions between 5 and 10 nm.

Based on the experimental results, Figure 8 illustrates a possible formation mechanism of CNFs, CNTs and GNSs during the pyrolysis process. At high temperature, PMA is quickly decomposed into various pyrolytic species. Because the superior insulators formed by Oclay plallets could prevent pyrolytic species of PMA from escaping, more char residues are left.[36] As soon as the reductive pyrolytic species contact Fe_2O_3, Co_3O_4 and NiO, they are immediately reduced to Fe, Co, and Ni nanoparticles. The carbon atoms dissolution in the metal nanoparticles and the concomitant precipitation of solid carbon leads to the formation of graphitic layers, which will be evolved into various structures depending on factors such as the interaction between the metal and graphitic carbon, diameter of metal and the strain in the graphitic carbon.[37,38] The graphitic carbon atoms possessing weak interactions with Fe are assembled into dense 2D CNFs on the surface of Fe nanoparticles with large diameter similar to the growth on flat substrates.[39] Because of the strong interactions between graphitic carbon atoms and Co, Co nanoparticles with small diameters are deactivated through the complete covering by the graphitic carbon atoms and thus the core–shell nanospheres are eventually formed.[40] Maybe because the attractions with Ni nanoparticles can be partly overcome, so the graphitic carbon atoms grows in diameter and length to form 1D CNTs.[41]

CONCLUSION

This work presents a pyrolytic route for the selective synthesis of CNFs, CNSs, and CNTs by changing only the catalyst precursors. CNFs were produced when Fe_2O_3 was used as the catalyst, CNSs were obtained in the presence of Co_3O_4, and the incorporation of NiO led to the formation of CNTs. The as-prepared carbon materials are highly graphitized and contain few oxygen-containing groups on the surface. Fe, Co and Ni nanoparticles with high crystallinity, in situ formed from the reduction of their oxides by the pyrolytic species of PMA, were the real active sites for the formation of CNFs, CNSs, and CNTs, respectively. The route is simple and controllable for the selective preparation of carbon nanomaterials with a desired morphology.

ACKNOWLEDGMENTS

The research work is financially supported by National Basic Research Program of China (973 Program) (2012CB719701), the joint fund of NSFC and CAAC (No. 61079015), the Opening Project of State Key Laboratory of Fire Science of USTC (No. HZ2011-KF05), and the China Postdoctoral Science Foundation (2012M511418).

REFERENCES

1. Kroto, H. W.; Heath, J. R.; Obrien, S. C.; Curl, R. F.; Smalley, R. E. *Nature* **1985**, *318*, 162.
2. Liu, W. H.; Dang, T.; Xiao, Z. H.; Li, X.; Zhu, C. C.; Wang, X. L. *Carbon* **2011**, *49*, 884.
3. Nieto-Marquez, A.; Valverde, J. L.; Keane, M. A. *Appl. Catal. A Gen.* **2009**, *352*, 159.
4. Wong, S. S.; Joselevich, E.; Woolley, A.T.; Cheung, C. L.; Lieber, C. M. *Nature* **1998**, *394*, 52.
5. Verdejo, R.; Bernal, M. M.; Romasanta, L. J.; Lopez-Manchado, M. A. *J. Mater. Chem.* **2011**, *21*, 3301.
6. Qiu, J. J.; Wang, S. R. *J. Appl. Polym. Sci.* **2011**, *119*, 3670.
7. Zhou, X. W.; Zhu, Y. F.; Liang, L. *Mater. Res. Bull.* **2007**, *42*, 456.
8. Coleman, J. N.; Khan, U.; Blau, W. J.; Gun'ko, Y. K. *Carbon* **2006**, *44*, 1624.
9. Larsen, R. M. *J. Mater. Sci.* **2009**, *44*, 799.
10. Wu, Y. H.; Qiao, P. W.; Chong, T. C.; Shen, Z. X. *Adv. Mater.* **2002**, *14*, 64.
11. Wang, J. J.; Zhu, M. Y.; Outlaw, R. A.; Zhao, X.; Manos, D. M.; Holloway, B. C. *Carbon* **2004**, *42*, 2867.
12. Serp, P.; Feurer, R.; Kalck, P.; Kihn, Y.; Faria, J. L.; Figueiredo, J. L. *Carbon* **2001**, *39*, 615.
13. Wang, Z. L.; Kang, Z. C. *J. Phys. Chem.* **1996**, *100*, 17725.
14. Wang, Y.; Nepal, D.; Geckeler, K. E. *J. Mater. Chem.* **2005**, *15*, 1049.
15. Lyu, S. C.; Liu, B. C.; Lee, C. J. *Chem. Mater.* **2003**, *15*, 3951.
16. Hou, H. Q.; Schaper, A. K.; Weller, F.; Greiner, A. *Chem. Mater.* **2002**, *14*, 3990.
17. Liu, F.; Zhang, Y. *Carbon* **2010**, *48*, 2394.
18. Xu, Z. W.; Li, H. J.; Li, W.; Cao, G. X.; Zhang, Q. L.; Li, K. Z.; Fu, Q. G.; Wang, J. *Chem. Commun.* **2011**, *47*, 1166.
19. Sun, Z. Z.; Yan, Z,; Yao, J.; Beitler, E.; Zhu, Y.; Tour, J. M. *Nature* **2010**, *468*, 549.
20. Pol, S. V.; Pol, V. G.; Sherman, D.; Gedanken, A. *Green Chem.* **2009**, *11*, 448.
21. Xu, S.; Yan, X. B.; Wang, X. L.; Yang, S. R.; Xue, Q. J. *J. Mater. Sci.* **2010**, *45*, 2619.
22. Pol. V. G. *Environ. Sci. Technol.* **2010**, *44*, 4753.
23. Tang, T.; Chen, X. C.; Meng, X. Y.; Chen, H.; Ding, Y. P. *Angew. Chem. Int. Ed. Engl.* **2005**, *44*, 1517.
24. Song, R. J.; Li, B.; Zhao, S.; Li, L. P. *J. Appl. Polym. Sci.* **2009**, *112*, 3423.
25. Inagaki, M.; Fujita, K.; Takeuchi, Y.; Oshida, K.; Iwata, H.; Konno, H. *Carbon* **2001**, *39*, 921.
26. Qi, X. S.; Deng, Y.; Zhong, W.; Yang, Y.; Qin, C.; Au, C.; Du, Y. W. *J. Phys. Chem. C* **2010**, *114*, 808.
27. Jana, P.; O'Shea, V. A. D.; Coronado, J. M.; Serrano, D. P. *Energy Environ. Sci.* **2011**, *4*, 778.
28. Qian, W. Z.; Liu, T.; Wang, Z. W.; Yu, H.; Li, Z. F.; Wei, F. *Carbon* **2003**, *41*, 2487.
29. Sridhar, V.; Jeon, J. H.; Oh, I. K. *Carbon* **2010**, *48*, 2953.
30. Huang, Z. P.; Wang, D. Z.; Wen, J. G.; Sennett, M.; Gibson, H.; Ren, Z. F. *Appl. Phys. A* **2002**, *74*, 387.
31. Hong, N. N.; Yang, W.; Bao, C. L.; Jiang, S. H.; Song, L.; Hu, Y. *Mater. Res. Bull.* **2012**, *47*, 4082.

32. Zhang, W. X.; Cui, J. C.; Tao, C. A.; Wu, Y. G.; Li, Z. P.; Ma, L.; Wen, Y. Q.; Li, G. T. *Angew. Chem. Int. Ed. Engl.* **2009**, *48*, 5864.
33. Lee, Y. F.; Chang, K. H.; Hu, C. C. *Chem. Commun.* **2011**, *47*, 2297.
34. Lyon, R. E.; Walters, R. N.; Stoliarov, S. I. *Polym. Eng. Sci.* **2007**, *47*, 1501.
35. Zhu, J.; Start, P.; Mauritz, K. A.; Wilkie, C. A. *Polym. Degrad. Stabil.* **2002**, *77*, 253.
36. Cai, Y. B.; Hu, Y.; Song, L.; Xuan, S.Y.; Zhang, Y.; Chen, Z. Y.; Fan, W. C. *Polym. Degrad. Stabil.* **2007**, *92*:490.
37. Ding, F.; Rosen, A.; Campbell, E. E. B.; Falk, L. K. L.; Bolton, K. *J. Phys. Chem. B* **2006**, *110*, 7666.
38. Liu, Z. J.; Yuan, Z. Y.; Zhou, W. Z.; Xu, Z. D.; Peng, L. M. *Chem. Vapor Depos.* **2001**, *7*, 248.
39. John, R.; Ashokreddy, A.; Vijayan, C.; Pradeep, Y. *Nanotechnology* **2011**, *22*, 165701.
40. Chen, X. C.; Wang, H.; He, J. H. *Nanotechnology* **2008**, *19*, 325607.
41. Fernandez, Y.; Menendez, J. A.; Phillips, J.; Luhrs, C. *Appl. Surf. Sci.* **2009**, *256*, 194.